LAWRENCE
LIVERMORE
NATIONAL
LABORATORY

LLNL-CONF-418141

Modeling Heat Conduction and Radiation Transport with the Diffusion Equation in NIF ALE-AMR

A. C. Fisher, D. S. Bailey, T. B. Kaiser, B. T. N. Gunney, N. D. Masters, A. E. Koniges, D. C. Eder, R. W. Anderson

October 16, 2009

Inertial Fusion Sciences and Applications (IFSA)
San Francisco, CA, United States
September 6, 2009 through September 11, 2009

Disclaimer

Modeling Heat Conduction and Radiation Transport with the Diffusion Equation in NIF ALE-AMR

A.C. Fisher[1], D.S. Bailey[1], T.B. Kaiser[1], B.T.N. Gunney[1], N.D. Masters[1], A.E. Koniges[2], D.C. Eder[1], R.W. Anderson[1]

1: Lawrence Livermore National Laboratory, P.O.Box 808, Livermore, CA 94551, USA
2: Lawrence Berkeley National Laboratory, 1 Cyclotron Rd. Berkeley, CA 94720, USA

E-mail: fisher47@llnl.gov

Abstract. The ALE-AMR code developed for NIF is a multi-material hydro-code that models target assembly fragmentation in the aftermath of a shot. The combination of ALE (Arbitrary Lagrangian Eulerian) hydro with AMR (Adaptive Mesh Refinement) allows the code to model a wide range of physical conditions and spatial scales. The large range of temperatures encountered in the NIF target chamber can lead to significant fluxes of energy due to thermal conduction and radiative transport. These physical effects can be modeled approximately with the aid of the diffusion equation. We present a novel method for the solution of the diffusion equation on a composite mesh in order to capture these physical effects.

1. Introduction

This work is focused on improving the modeling capability for NIF debris and shrapnel simulations. Such simulations are being used by the NIF program to predict fragment sizes and velocities in the aftermath of a NIF target shot. This capability allows us to detect fragments that may damage NIF optics and diagnostics beforehand and redesign targets in order to reduce such risks before NIF target shots are taken.

In this paper we present recent progress in adding heat conduction and radiation transport effects to the ALE-AMR code. In order to add these effects an AMR (Adaptive Mesh Refinement) capable diffusion solver is required. We will describe our diffusion solver and the testing we used to show that it is $2nd$ order accurate. We will also describe the work required to introduce heat conduction and radiation transport modules into ALE-AMR. Finally, we will present a demonstration simulation using these new capabilities.

2. AMR Capable Finite Element Diffusion Solver

To work with ALE-AMR our diffusion solver must be capable of operating on the multi-level, multi-processor, block structured SAMRAI data representing the ALE-AMR variables. The Finite Element Method (FEM), however, requires data in a single level composite mesh format. Also after the solution is obtained in the composite mesh format it must be used to update the ALE-AMR data in the multi-level format. This necessitates a mapping capable of translating between the SAMRAI representation and the composite mesh representation.

To begin forming this mapping we detect which nodes in the SAMRAI representation are at the finest level for that location and thus need to be nodes in the composite mesh. For each

finest node that is detected a unique, non-contiguous fine ID number can be computed using the index of the node and vice versa as follows

$$\begin{aligned} F &= i + jN_i + kN_iN_j \\ i = F\%N_i,\ j &= (F/N_i)\%N_j,\ k = F/(N_iN_j) \end{aligned} \tag{1}$$

where (i, j, k) is the SAMRAI index location of the node assuming it was refined to the finest level and (N_i, N_j, N_k) is the number of nodes in each direction assuming the entire block was refined to the finest level. Every unique node is then counted in sequence to yield a contiguous global ID numbering for the nodes. A map between this contiguous global ID number and the non-contiguous fine ID number is constructed and stored for later use. When more than one CPU is used each CPU counts the nodes it owns and the numbers are shifted by the number of nodes owned by the lower numbered CPUs. For nodes that are shared by more than one CPU in the SAMRAI representation, a tie breaker is used to determine which CPU owns the node and all the other CPUs sharing the node store the global ID in another map for later use. These maps and (1) allow straightforward translation between indices in the SAMRAI representation and global ID numbers for the composite mesh representation.

In addition to this translation between representations, a family of finite elements is required to handle all of the cases found in the composite mesh. For elements that are not at a coarse-fine boundary, standard bilinear quads in $2D$ and trilinear hexes in $3D$ are used. However, there are many cases of elements at the coarse-fine boundary with each case having a different combination of element faces refined. For these elements we use an approach similar to the transition elements found in [1]. The extra nodes on the faces due to the transition have hat basis functions along that face with the value reaching 1 at that node and 0 at the other nodes on the face. In the dimension not on the face the basis function is simply linear. The corner basis functions in our transition elements are the standard linear functions with fractions of the new transition basis functions subtracted out in order to ensure that the corner basis function is 0 at all the transition nodes. This method of construction yields a set of basis functions that satisfies the interpolation property and also enforces continuity across all the element faces.

Using the composite mesh mapping and the family of transition elements it is now possible to apply the FEM within the framework of ALE-AMR. We now turn our attention to the solution of the following diffusion equation.

$$\nabla \cdot \delta \nabla u + \sigma u = f \tag{2}$$

Applying the standard Galerkin approach yields the following linear system approximation

$$\begin{aligned} A\mathbf{u} + \mathbf{b} &= \mathbf{f} \\ A &= M_\sigma - K_\delta \\ (M_\alpha)_{ij} &= \textstyle\int_\Omega \alpha \phi_i \phi_j d\Omega \\ (K_\alpha)_{ij} &= \textstyle\int_\Omega \alpha \nabla \phi_i \cdot \nabla \phi_j d\Omega \\ \mathbf{b} &= 0 \end{aligned} \tag{3}$$

where M is the mass matrix, K is the stiffness matrix, and an insulating boundary means $\mathbf{b} = 0$. A set of quadrature rules is needed to approximate the integrals and construct the matrices. For the standard elements we use a basic mass lumping integration rule with quadrature points located at the corners of the element. Using this quadrature rule generates an A matrix that has the M-matrix property and thus is inverse positive. Inverse positivity is an important property for physical models such as heat conduction since temperatures are expected to stay above absolute zero. For the transition elements a set of mass lumping quadrature rules is constructed by evaluating points at every node location in the element including the corner nodes and the nodes on the transition faces. Unfortunately the gradient of the transition basis functions is

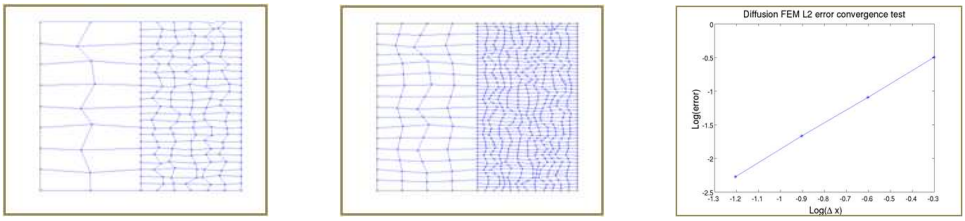

Figure 1. Convergence test on a mesh with transition elements indicates 2nd order accuracy.

undefined at the transition node locations. We step around this problem by taking the limits of the gradient from each distinct region touching the point (2 in $2D$ and 4 in $3D$) and averaging those limits. This allows the formation of lumped mass and stiffness matrices found in (3). That linear system is solved by using the HYPRE library providing an approximate solution to the diffusion equation.

We measure the accuracy of this solution using a standard L_2 error convergence test. A randomized mesh is generated with the right side refined using a ratio of 3:1 in order to test the transition elements Figure 1. The entire random mesh is then refined 3 more times yielding a total of 4 meshes. Each of these meshes is used to approximate the solution to a simple Possion problem with non-zero Dirichlet boundary. These approximations are then compared to the analytical result to obtain the L_2 norm of the error. The behavior of these error norms, shown in Figure 1, indicates that the method has 2nd order convergence.

3. Heat Conduction and Radiation Transport Modeling

Now that we have a diffusion equation solver, both heat conduction and radiation transport can be modeled with relative ease. For heat conduction the equation can be time evolved implicitly by using the solver at each time step yielding

$$\begin{aligned} C_v \tfrac{T^{n+1}-T^n}{\Delta t} &= \nabla \cdot D^n \nabla T^{n+1} - \alpha T^{n+1} \\ \delta = D^n,\ \sigma = -\alpha - \tfrac{C_v}{\Delta t} T^n,\ f &= -\tfrac{C_v}{\Delta t} T^n \end{aligned} \tag{4}$$

where C_v is the specific heat, T is temperature represented at the nodes, D is the heat conductivity, and α is the absorptivity. The variables δ, σ, and f are the diffusion equation parameters from (2). Similarly the diffusion approximation to radiation transport can be implicitly time evolved yielding

$$\begin{aligned} \tfrac{E_R^{n+1}-E_R^n}{\Delta t} &= \nabla \cdot \lambda(\tfrac{c}{\kappa_r}) \nabla E_R^{n+1} + \tilde{\kappa}_p (B^n - c E_R^{n+1}) \\ C_v \tfrac{T^{n+1}-T^n}{\Delta t} &= -\tilde{\kappa}_p (B^n - c E_R^{n+1}) \\ \delta = \lambda(\tfrac{c}{\kappa_r}),\ \sigma = -\tilde{\kappa}_p c - \tfrac{1}{\Delta t},\ f &= -\tfrac{1}{\Delta t} - \tilde{\kappa}_p B^n \end{aligned} \tag{5}$$

where E_R is the radiation energy represented at the nodes, λ is a function used to impose flux limiting on the diffusion approximation, c is the speed of light, κ_r is the Rosseland opacity, $\tilde{\kappa}_P$ is a modification to Planck opacity which is used to linearize the equation as in [2], and B is the blackbody intensity. After E_R and T are evolved through the above equations, the material temperatures and energies must be updated to reflect the changes. However, in ALE-AMR the material temperatures and energies are represented at the cell centers and not the nodal values which are being updated by the heat conduction and radiation transport. A method for mapping variables from nodes to cell centers and back is needed to couple the hydro variables with nodal variables used in the diffusion solver. We chose the method described by [3] in which changes in variables are mapped between nodes and cells. These mappings make it possible to transfer energy between nodes and cells without introducing large amounts of artificial diffusion.

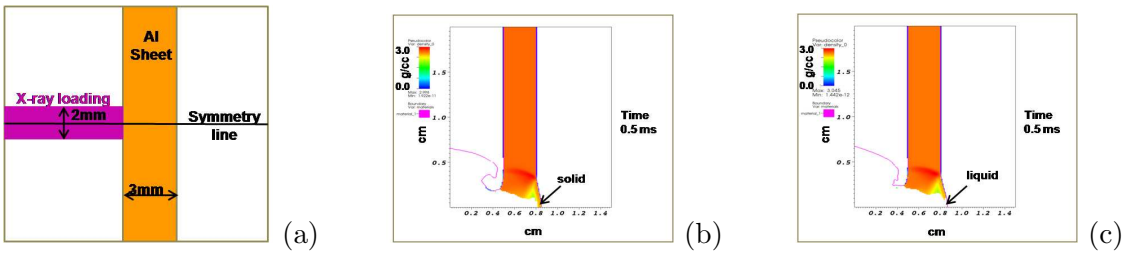

Figure 2. (a) Setup for an Al X-Ray interaction simulation. A $10^5 J/cm^2$ source of X-Rays was loaded onto the surface of an Al foil. (b,c) Density of remaining solid Al after 0.5 μs without and with radiation transport effects respectively.

4. Simulation Results

To demonstrate this new capability in ALE-AMR we chose a simulation related to the NIF debris and shrapnel work. In these $2D$ simulations a $1ns$ $10^5 J/cm^2$ x-ray pulse was loaded onto $2mm$ of the surface of a $3mm$ thick Al foil. The simulations were allowed to run to $0.5\mu s$ both with and without the new radiation transport module active. At the end of the simulations we captured density plots of the Al, and thresholded those densities by the material state. All of the Al that had a temperature above the melting point was thresholded to white while all of the Al that was still solid was drawn with the color scale (see Figure 2). While the differences between the simulations appear small they are still significant. In the simulation without radiation transport the foil appears ready to spall off solid material from the back side. In the simulation with radiation transport the material coming off the back side has melted which means it will be more likely to break into smaller droplets in transit to any optics or diagnostics. The droplets are a lower debris risk which is exactly what we are tasked to measure for NIF targets. This highlights the importance of modeling radiation transport to the NIF debris and shrapnel project.

5. Conclusions

The ALE-AMR code is now capable of modeling heat conduction and radiation transport effects. In order to model these effects in the ALE-AMR framework an AMR capable FEM diffusion solver was developed. This diffusion solver was put through an L_2 error convergence test to show that it is $2nd$ order accurate. Heat conduction and Radiation Transport modules were developed using this diffusion solver and a technique for mapping variables from cells to nodes and vice versa. Also an X-Ray Al foil interaction was simulated with and without radiation transport effects, highlighting the importance of radiation transport to the NIF debris and shrapnel work.

Acknowledgments

This work performed under the auspices of the U.S. Department of Energy by Lawrence Livermore National Laboratory under Contract DE-AC52-07NA27344

References

[1] Gupta A 1978 *International Journal for Numerical Methods in Engineering* **12** 35–45
[2] Shestakov A, Harte J and Kershaw D 1988 *Journal of Computational Physics* **76** 385–413
[3] Shestakov A, Milovich J and Prasad M 2001 *Journal of Computational Physics* **170** 81–111